symmetry

MDPI

Article

Heat and Mass Transfer on Magnetohydrodynamics Casson Carbon Nanotubes Nanofluid Flow in an Asymmetrical Channel via Porous Medium

Wan Nura'in Nabilah Noranuar, Ahmad Qushairi Mohamad *, Sharidan Shafie and Lim Yeou Jiann

Department of Mathematical Sciences, Faculty of Science, Universiti Teknologi Malaysia, Johor Bahru 81310, Johor, Malaysia; wannurainnabilah189@gmail.com (W.N.N.N.); sharidan@utm.my (S.S.); jiann@utm.my (L.Y.J.)

* Correspondence: ahmadqushairi@utm.my

Abstract: The rapid development of nanotechnology in our emerging industries has drawn the interest of numerous researchers and scientists, especially in experimental and numerical studies. Therefore, the present analytical study will help reduce time and costs and validate the numerical study. However, the analytical research of carbon nanotubes with Casson fluid in a channel is still limited. Therefore, the current analytical study inspected the consequences of carbon nanotubes (CNTs) nanoparticles on the heat and mass transfer of magnetohydrodynamics (MHD) Casson nanofluid flow induced by a moving vertical plate with a porous region inside an asymmetrical channel. Dimensional governing equations are used for the modelling, which is then expressed in a dimensionless form by employing dimensionless variables. The analytical solutions for the velocity, temperature, and concentration are tackled using the Laplace transform technique. The temperature and velocity are significantly enhanced when increasing the nanoparticle volume fraction. This is due to the outstanding characteristic of nanofluid thermal conductivity, which results in an efficient heat transfer. This result has the potential to be applied to various nanofluid cooling technologies. Since the solutions are determined in an analytical form, this study could be used as a reference for other numerical and experimental works and a guide for several industries.

Keywords: Casson nanofluid; porosity; magnetohydrodynamics; heat and mass transfer; Laplace transform

Citation: Noranuar, W.N.N.; Mohamad, A.Q.; Shafie, S.; Jiann, L.Y. Heat and Mass Transfer on Magnetohydrodynamics Casson Carbon Nanotubes Nanofluid Flow in an Asymmetrical Channel via Porous Medium. *Symmetry* **2023**, *15*, 946. https://doi.org/10.3390/sym15040946

Academic Editor: Iver H. Brevik

Received: 15 March 2023
Revised: 8 April 2023
Accepted: 17 April 2023
Published: 20 April 2023

1. Introduction

Many modern technologies, especially those that involve energy conversion, chemical processing, and material synthesis, rely on diffusion heat and mass transfer (double-diffusive). In response to today's concerns with energy generation and its environmental impact, numerous researchers have broadened their discussion on the heat- and mass-transfer phenomenon. Notable amongst them are Pattnaik et al. [1] and Rao et al. [2], who investigated heat and mass transfer in an unsteady radiative flow beyond an exponentially accelerated plate. Mohamad et al. [3] and Noranuar et al. [4] explored the flow features of non-coaxial rotating viscous fluid under the influence of heat and mass transfer. Zulkiflee et al. [5] studied a radiated sine and cosine oscillatory convective flow within two parallel plates with heat- and mass-transfer analysis. A series of studies discussing the transportation of thermal and mass in a convective flow can be found in the study of Sehra et al. [6], Abbas et al. [7], Riaz et al. [8], and Afridi et al. [9].

Recent advances have augmented the complementary of the double diffusive phenomenon with a new discussion of nanofluid. Nanofluid is familiar with the upgraded thermal conductivity of conventional base fluid that is affected by the suspension of nano-scale particles (nanoparticles). A fundamental study of double diffusive nanofluid flow was performed by Mahanthesh et al. [10] using a water-based copper nanofluid. A moving

vertical plate is imposed to induce a fluid flow. Madhura et al. [11] worked on a similar double-diffusive nanofluid study, but the fluid flow was generated by imposing an exponentially accelerated plate. With the aid of the Laplace transform, Farooq et al. [12] computed the exact solution for the heat and mass transport of Maxwell nanofluid over an oscillating vertical plate. Siddique et al. [13] carried out an analytical study with the help of the Laplace transform to investigate the transmission of thermal and solutal in a channel for a radiated Casson nanofluid flow without a magnetic field and porosity effects. Arulmozhi et al. [14] examined a chemically reacting flow of radiative nanofluid across a moving plate with a double diffusion analysis. In addition to the advancement of nanofluid, carbon nanotubes (CNTs) serve as the most attractive candidate for a wide range of applications due to their excellent properties: a high electrical and thermal conductivity. Prabavathi et al. [15] and Sreedevi et al. [16] explored the fluid-flow features of using water-based CNTs nanofluid in a vertical cone with the effects of MHD. Utilizing a similar nanofluid, Reddy and Reddy [17] analyzed the transportation of heat and mass in a porous medium bounded by an inclined plate. Javed et al. [18] explored the influences of CNTs nanoparticles on the double diffusion of chemically reacting second-grade fluid in porous material. Noranuar et al. [19] scrutinized the double-diffusive flow of rotating Casson nanofluid using human-blood-based carbon nanotubes as the nanofluid, with the flow being generated by a moving plate. Based on these studies, no study has conducted a double-diffusive flow of Casson CNTs nanofluid incorporated with both MHD and porosity effects in a channel.

The magnetohydrodynamics (MHD) effect is a physical phenomenon describing the motion of a conducting fluid flowing under the influence of an external magnetic field. The controlling double-diffusive phenomenon by means of MHD has been found in many practical applications. In medical research and biological systems, magnetic medication targeting, changing blood flow during surgery, cancer tumor therapy, carrying complicated bio-waste fluid, and magnetic endoscopy are all applications of MHD. In this case, MHD becomes significant as its imposition produces an applied force and acts as a heat supplier. Meanwhile, the porosity of a porous medium elucidates the fraction of void space in the material, where the void may contain air or water. It is evaluated as a fraction between 0 and 1 or a percentage between 0% and 100%. The modelling of the transport phenomenon embedded in porous media is also practicable in biological systems, as a biological structure (i.e., tissue) can be viewed as a blood-saturated porous matrix comprising interstices and cells. The investigation of the MHD flow of an incompressible nanofluid via porous material in a channel is carried out by Saqib et al. [20] by using CMC-based CNTs nanofluid. Kumar et al. [21] used water-based Al_2O_3 nanofluid to explore the MHD effect on a convective flow over a stretching sheet. Rehman et al. [22] and Ali et al. [23] investigated the interaction of MHD in nanofluid using a numerical approach. Without nanoparticle impacts, Ramzan et al. [24] examined a generalized MHD flow in porous medium for Casson fluid via a channel in the presence of mass and heat transport. Azmi et al. [25] investigated heat transfer and MHD Casson fluid flow beyond a channel without nanoparticles and porosity effects. Excluding the porosity effect, Sadiq et al. [26] investigated double-diffusion flow in a channel for a MHD Casson nanofluid with a stationary plate. By considering the effect of MHD, porosity, and heat and mass transfer, Asifa et al. [27] studied a convective flow of Casson fluid bounded in a channel. In keeping with the aforementioned review, there is no study that discusses the heat- and mass-transfer phenomenon for an incompressible Casson fluid, particularly under the influences of CNTs nanoparticles, MHD, and porosity in a channel with a moving plate. Therefore, the present study investigates a double-diffusion MHD flow in an asymmetrical channel for a Casson-based CNTs nanofluid saturated in a porous medium with a moving plate as its flow simulator. The problem is represented by governing equations consisting of momentum, energy, and concentration equations, together with initial and boundary conditions. The dimensionless variables are substituted into the equations to produce pertinent dimensionless parameters. The investigation is settled using the transformation of Laplace. The effects of the parameters

on the velocity, temperature, and concentration are then plotted using Mathcad. The results of this analytical study could be used as a benchmark for numerical and experimental studies, as well as a reference for the education and industry sectors.

2. Mathematical Formulation

The flow of an electrically conductive Casson nanofluid within an asymmetrical channel driven by a moving vertical plate at $y = 0$ is considered, as depicted clearly in Figure 1. The nanofluid is composed of the synthesis of SWCNTs and MWCNTs, respectively, in human blood, and it flows unsteadily through a porous medium with the effects of heat and mass transfer. The channel is made up of two parallels with a distance of h and infinitely vertical plates, positioned in an upward direction along the x-axis, while the normal to the plane of the plate is along the y-axis. A transverse magnetic field of uniform strength B_0 is applied perpendicularly to the x-axis. At $t = 0$, both the fluid and plates are in a stationary state with a constant temperature and concentration, T_h and C_h. After $t > 0$, the plate at $y = 0$ begins to move with a velocity u_0, the temperature and concentration of the fluid are raised to T_w and C_w, causing the buoyancy force to be enhanced, and the fluid starts to move in the x-direction with free-convection phenomena. The length of the channel's walls is infinite; all the physical quantities depend on y and t only. Under this assumption, with the use of the usual Boussinesq approximation [23], the problem is governed by the following equations [2,13].

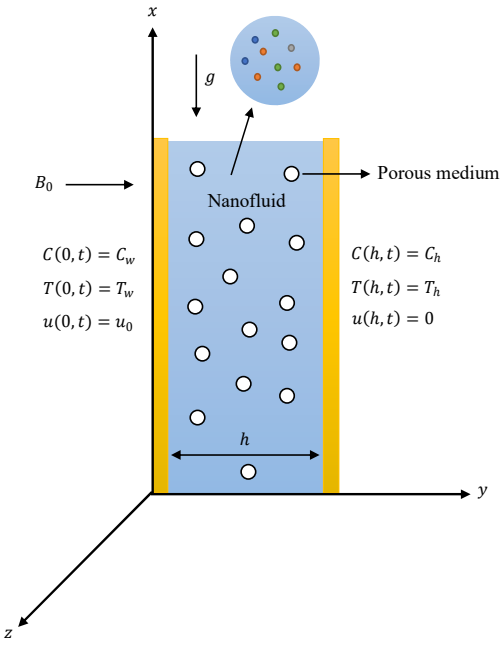

Figure 1. Problem configuration.

Momentum equation:

$$\rho_{nf}\frac{\partial \widetilde{u}}{\partial \widetilde{t}} = \mu_{nf}\left(1+\frac{1}{\gamma}\right)\frac{\partial^2 \widetilde{u}}{\partial \widetilde{y}^2} - \sigma_{nf}{B_0}^2\widetilde{u} - \frac{\mu_{nf}}{k_1}\widetilde{u} + (\rho\beta_T)_{nf}g\left(\widetilde{T}-\widetilde{T}_h\right) + (\rho\beta_C)_{nf}g\left(\widetilde{C}-\widetilde{C}_h\right), \quad (1)$$

Energy equation:

$$\left(\rho C_p\right)_{nf}\frac{\partial \widetilde{T}}{\partial \widetilde{t}} = k_{nf}\frac{\partial^2 \widetilde{T}}{\partial \widetilde{y}^2}, \quad (2)$$

Concentration equation:

$$\frac{\partial \widetilde{C}}{\partial \widetilde{t}} = D_{nf}\frac{\partial^2 \widetilde{C}}{\partial \widetilde{y}^2}, \quad (3)$$

where $\gamma = \mu\sqrt{2\pi_c}/p_y$ is the Casson parameter, $u(y,t)$, $T(y,t)$, and $C(y,t)$ are the velocity, temperature, and concentration for nanofluid, and k_1 and g are the permeability of the porous medium and acceleration due to gravity. Since the problem is considered as a free-convection problem, the term "g" is considered in our governing equation (Equation (1)). Based on the definition of free convection, the movement of fluid is only generated by density differences in the fluid occurring due to temperature gradients and a gravitational field without external forces. Meanwhile, ρ_{nf}, μ_{nf}, σ_{nf}, $(\beta_T)_{nf}$, $(\beta_C)_{nf}$, $(C_p)_{nf}$, k_{nf}, and D_{nf} are the nanofluid constants for the density, dynamic viscosity, electric conductivity, thermal expansion coefficient, concentration expansion coefficient, specific heat, thermal conductivity, and mass diffusivity, as shown in Equation (7) [19]. The thermophysical properties used in this study are found in Table 1.

Table 1. Thermophysical properties for human blood, SWCNTs, and MWCNTs.

	$\rho(\mathbf{Kgm^{-3}})$	$C_p(\mathbf{JKg^{-1}K^{-1}})$	$k(\mathbf{Wm^{-1}K^{-1}})$	$\sigma(\mathbf{Sm^{-1}})$	$\beta\times\mathbf{10^{-1}}(\mathbf{K^{-1}})$
Human blood	1053	3594	0.492	0.8	0.18
SWCNTs	2600	425	6600	10^6–10^7	27
MWCNTs	1600	796	3000	1.9×10^{-4}	44

The prescribed conditions for the initial and boundary are shown in Equations (4)–(6).

$$\widetilde{u}\left(\widetilde{y},0\right) = 0;\ \widetilde{T}\left(\widetilde{y},0\right) = \widetilde{T}_h;\ \widetilde{C}\left(\widetilde{y},0\right) = \widetilde{C}_h;\ \forall 0 \le \widetilde{y} \le h, \frac{\partial \widetilde{C}}{\partial \widetilde{t}} = D_{nf}\frac{\partial^2 \widetilde{C}}{\partial \widetilde{y}^2}, \tag{4}$$

$$\widetilde{u}\left(0,\widetilde{t}\right) = u_0;\ \widetilde{T}\left(0,\widetilde{t}\right) = \widetilde{T}_w;\ \widetilde{C}\left(0,\widetilde{t}\right) = \widetilde{C}_w;\ \forall \widetilde{t} \ge 0, \tag{5}$$

$$\widetilde{u}\left(h,\widetilde{t}\right) = 0;\ \widetilde{T}\left(h,\widetilde{t}\right) = \widetilde{T}_h;\ \widetilde{C}\left(h,\widetilde{t}\right) = \widetilde{C}_h;\ \forall \widetilde{t} \ge 0. \tag{6}$$

$$\begin{gathered}
\rho_{nf} = (1-\phi)\rho_f + \phi\rho_{CNTs},\ \mu_{nf} = \frac{\mu_f}{(1-\phi)^{2.5}}, \\
\sigma_{nf} = 1 + \frac{3\left(\frac{\sigma_{CNTs}}{\sigma_f}-1\right)\phi}{\left(\frac{\sigma_{CNTs}}{\sigma_f}+2\right)-\phi\left(\frac{\sigma_{CNTs}}{\sigma_f}-1\right)}, \\
\beta_{nf} = \frac{(1-\phi)(\rho\beta)_{nf}+\phi(\rho\beta)_{CNTs}}{\rho_{nf}},\ (C_p)_{nf} = \frac{(1-\phi)(\rho C_p)_f+\phi(\rho C_p)_{CNTs}}{\rho_{nf}}, \\
\frac{k_{nf}}{k_f} = \frac{1-\phi+2\phi\frac{k_{CNTs}}{k_{CNTs}-k_f}\ln\frac{k_{CNTs}+k_f}{2k_f}}{1-\phi+2\phi\frac{k_f}{k_{CNTs}-k_f}\ln\frac{k_{CNTs}+k_f}{2k_f}},\ D_{nf} = (1-\phi)D_f.
\end{gathered} \tag{7}$$

Employing the following dimensionless variables,

$$u = \frac{\widetilde{u}}{u_0},\ y = \frac{\widetilde{y}}{h},\ t = \frac{\widetilde{t}\,v_f}{h^2},\ T = \frac{\widetilde{T}-\widetilde{T}_h}{\widetilde{T}_w-\widetilde{T}_h},\ C = \frac{\widetilde{C}-\widetilde{C}_h}{\widetilde{C}_w-\widetilde{C}_h}, \tag{8}$$

Equations (1)–(3) with their conditions (4) to (6), incorporated into Equation (7), turn into the following dimensionless expression:

$$\frac{\partial u}{\partial t} = \frac{1}{b_5}\frac{\partial^2 u}{\partial y^2} - b_2 Mu - \frac{b_1}{K}u + b_3 GrT + b_4 GmC, \tag{9}$$

$$\frac{\partial T}{\partial t} = \frac{1}{a_1}\frac{\partial^2 T}{\partial y^2}, \tag{10}$$

$$\frac{\partial C}{\partial t} = \frac{1}{a_2}\frac{\partial^2 C}{\partial y^2}, \tag{11}$$

$$u(y,0) = 0;\ T(y,0) = 0;\ C(y,0) = 0;\ \forall 0 \le y \le 1, \tag{12}$$

$$u(0,t) = 1;\ T(0,t) = 1;\ C(y,0) = 1;\ \forall t \ge 0, \tag{13}$$

$$u(1,t) = 0;\ T(1,t) = 0;\ C(1,0) = 0;\ \forall t \ge 0, \tag{14}$$

where:

$$a_1 = \frac{\Pr\phi_4}{\lambda}, a_2 = \frac{Sc}{1-\phi}, b_1 = \frac{\phi_1}{\phi_2}, b_2 = \frac{\sigma}{\phi_2}, b_3 = \frac{\phi_3}{\phi_2}, b_4 = \frac{\phi_5}{\phi_2},$$
$$b_5 = \frac{1}{b_1}\left(\frac{\gamma}{\gamma+1}\right), \phi_1 = \frac{1}{(1-\phi)^{2.5}}, \phi_2 = (1-\phi) + \phi\frac{\rho_{CNTs}}{\rho_f},$$
$$\phi_3 = (1-\phi) + \phi\frac{(\rho\beta_T)_{CNTs}}{(\rho\beta_T)_f}, \phi_4 = (1-\phi) + \phi\frac{(\rho C_p)_{CNTs}}{(\rho C_p)_f},$$
$$\phi_5 = (1-\phi) + \phi\frac{(\rho\beta_C)_{CNTs}}{(\rho\beta_C)_f},$$

are constant parameters. The dimensionless parameters are the Prandtl number Pr, Schmidt number Sc, magnetic field M, porosity K, Grashof number Gr, and modified Grashof number Gm, expressed as [13,20]:

$$\Pr = \frac{(\rho C_p)_f v_f}{k_f},\ Sc = \frac{v_f}{D_f},\ M = \frac{\sigma_f {B_0}^2 h^2}{\mu_f},\ K = \frac{k_1}{h^2},$$
$$Gr = \frac{g(\beta_T)_f h^2 (T_w - T)}{u_0 v_f},\ Gm = \frac{g(\beta_C)_f h^2 (C_w - C)}{u_0 v_f}.$$

3. Problem Solution

Equations (9)–(14) are imposed with the Laplace transform, which gives:

$$\frac{d^2}{dy^2}\bar{u}(y,s) - \left(b_5 s + b_6 M + \frac{b_7}{K}\right)\bar{u}(y,s) = -b_8 Gr\bar{T}(y,s) - b_9 Gm\bar{C}(y,s), \tag{15}$$

$$\frac{d^2}{dy^2}\bar{T}(y,s) - a_1 s\bar{T}(y,s) = 0, \tag{16}$$

$$\frac{d^2}{dy^2}\bar{C}(y,s) - a_2 s\bar{C}(y,s) = 0, \tag{17}$$

$$\bar{u}(0,s) = \bar{T}(0,s) = \bar{C}(0,s) = \frac{1}{s}, \tag{18}$$

$$\bar{u}(1,s) = \bar{T}(1,s) = \bar{C}(1,s) = 0. \tag{19}$$

Then, the boundary conditions (18) and (19) are used to solve Equations (15)–(17). Lastly, with the use of inverse Laplace, the closed form of the velocity, temperature, and concentration are acquired accordingly, as follows:

$$\begin{aligned} u(y,t) = -u_1(y,t) \quad & +u_2(y,t) - u_3(y,t) + u_4(y,t) - u_5(y,t) + u_6(y,t) \\ & -u_7(y,t) + u_8(y,t) - u_9(y,t) + u_{10}(y,t) - u_{11}(y,t) \\ & +u_{12}(y,t) + u_{13}(y,t) - u_{14}(y,t) - u_{15}(y,t) + u_{16}(y,t) \\ & +u_{17}(y,t) - u_{18}(y,t), \end{aligned} \tag{20}$$

$$T(y,t) = \sum_{n=0}^{\infty}\left[erfc\left(\frac{2n+y}{2}\sqrt{\frac{a_1}{t}}\right) - erfc\left(\frac{2n+2-y}{2}\sqrt{\frac{a_1}{t}}\right)\right], \tag{21}$$

$$C(y,t) = \sum_{n=0}^{\infty}\left[erfc\left(\frac{2n+y}{2}\sqrt{\frac{a_2}{t}}\right) - erfc\left(\frac{2n+2-y}{2}\sqrt{\frac{a_2}{t}}\right)\right], \tag{22}$$

with

$$u_1(y,t) = \sum_{n=0}^{\infty}\left[\tfrac{1}{2}\exp\left(d_5\sqrt{b_{11}}\right)erfc\left(\tfrac{d_5}{2\sqrt{t}} + \sqrt{b_{11}t}\right) + \tfrac{1}{2}\exp\left(-d_5\sqrt{b_{11}}\right)erfc\left(\tfrac{d_5}{2\sqrt{t}} - \sqrt{b_{11}t}\right)\right],$$

$$u_2(y,t) = \sum_{n=0}^{\infty}\left[\tfrac{Gr_2}{2}\exp\left(d_5\sqrt{b_{11}}\right)erfc\left(\tfrac{d_5}{2\sqrt{t}} + \sqrt{b_{11}t}\right) + \tfrac{Gr_2}{2}\exp\left(-d_5\sqrt{b_{11}}\right)erfc\left(\tfrac{d_5}{2\sqrt{t}} - \sqrt{b_{11}t}\right)\right],$$

$$u_3(y,t) = \sum_{n=0}^{\infty}\left[\tfrac{Gr_2}{2}\exp\left(d_3t + d_5\sqrt{b_{11}+d_3}\right)erfc\left(\tfrac{d_5}{2\sqrt{t}} + \sqrt{(b_{11}+d_3)t}\right) + \tfrac{Gr_2}{2}\exp\left(d_3t - d_5\sqrt{b_{11}+d_3}\right)erfc\left(\tfrac{d_5}{2\sqrt{t}} - \sqrt{(b_{11}+d_3)t}\right)\right],$$

$$u_4(y,t) = \sum_{n=0}^{\infty}\left[\tfrac{Gm_2}{2}\exp\left(d_5\sqrt{b_{11}}\right)erfc\left(\tfrac{d_5}{2\sqrt{t}} + \sqrt{b_{11}t}\right) + \tfrac{Gm_2}{2}\exp\left(-d_5\sqrt{b_{11}}\right)erfc\left(\tfrac{d_5}{2\sqrt{t}} - \sqrt{b_{11}t}\right)\right],$$

$$u_5(y,t) = \sum_{n=0}^{\infty}\left[\tfrac{Gm_2}{2}\exp\left(d_4t + d_5\sqrt{b_{11}+d_4}\right)erfc\left(\tfrac{d_5}{2\sqrt{t}} + \sqrt{(b_{11}+d_4)t}\right) + \tfrac{Gm_2}{2}\exp\left(d_4t - d_5\sqrt{b_{11}+d_4}\right)erfc\left(\tfrac{d_5}{2\sqrt{t}} - \sqrt{(b_{11}+d_4)t}\right)\right],$$

$$u_6(y,t) = \sum_{n=0}^{\infty}\left[\tfrac{1}{2}\exp\left(d_6\sqrt{b_{11}}\right)erfc\left(\tfrac{d_6}{2\sqrt{t}} + \sqrt{b_{11}t}\right) + \tfrac{1}{2}\exp\left(-d_6\sqrt{b_{11}}\right)erfc\left(\tfrac{d_6}{2\sqrt{t}} - \sqrt{b_{11}t}\right)\right],$$

$$u_7(y,t) = \sum_{n=0}^{\infty}\left[\tfrac{Gr_2}{2}\exp\left(d_6\sqrt{b_{11}}\right)erfc\left(\tfrac{d_6}{2\sqrt{t}} + \sqrt{b_{11}t}\right) + \tfrac{Gr_2}{2}\exp\left(-d_6\sqrt{b_{11}}\right)erfc\left(\tfrac{d_6}{2\sqrt{t}} - \sqrt{b_{11}t}\right)\right],$$

$$u_8(y,t) = \sum_{n=0}^{\infty}\left[\tfrac{Gr_2}{2}\exp\left(d_3t + d_6\sqrt{b_{11}+d_3}\right)erfc\left(\tfrac{d_6}{2\sqrt{t}} + \sqrt{(b_{11}+d_3)t}\right) + \tfrac{Gr_2}{2}\exp\left(d_3t - d_6\sqrt{b_{11}+d_3}\right)erfc\left(\tfrac{d_6}{2\sqrt{t}} - \sqrt{(b_{11}+d_3)t}\right)\right],$$

$$u_9(y,t) = \sum_{n=0}^{\infty}\left[\tfrac{Gm_2}{2}\exp\left(d_6\sqrt{b_{11}}\right)erfc\left(\tfrac{d_6}{2\sqrt{t}} + \sqrt{b_{11}t}\right) + \tfrac{Gm_2}{2}\exp\left(-d_6\sqrt{b_{11}}\right)erfc\left(\tfrac{d_6}{2\sqrt{t}} - \sqrt{b_{11}t}\right)\right],$$

$$u_{10}(y,t) = \sum_{n=0}^{\infty}\left[\tfrac{Gm_2}{2}\exp\left(d_4t + d_6\sqrt{b_{11}+d_4}\right)erfc\left(\tfrac{d_6}{2\sqrt{t}} + \sqrt{(b_{11}+d_4)t}\right) + \tfrac{Gm_2}{2}\exp\left(d_4t - d_6\sqrt{b_{11}+d_4}\right)erfc\left(\tfrac{d_6}{2\sqrt{t}} - \sqrt{(b_{11}+d_4)t}\right)\right],$$

$$u_{11}(y,t) = \sum_{n=0}^{\infty}\left[Gr_2 erfc\left(\frac{d_7}{2\sqrt{t}}\right)\right],$$

$$u_{12}(y,t) = \sum_{n=0}^{\infty}\left[\tfrac{Gr_2}{2}\exp\left(d_3t + d_7\sqrt{d_3}\right)erfc\left(\tfrac{d_7}{2\sqrt{t}} + \sqrt{d_3t}\right) + \tfrac{Gr_2}{2}\exp\left(d_3t - d_7\sqrt{d_3}\right)erfc\left(\tfrac{d_7}{2\sqrt{t}} - \sqrt{d_3t}\right)\right],$$

$$u_{13}(y,t) = \sum_{n=0}^{\infty}\left[Gr_2 erfc\left(\frac{d_8}{2\sqrt{t}}\right)\right],$$

$$u_{14}(y,t) = \sum_{n=0}^{\infty}\left[\tfrac{Gr_2}{2}\exp\left(d_3t + d_8\sqrt{d_3}\right)erfc\left(\tfrac{d_8}{2\sqrt{t}} + \sqrt{d_3t}\right) + \tfrac{Gr_2}{2}\exp\left(d_3t - d_8\sqrt{d_3}\right)erfc\left(\tfrac{d_8}{2\sqrt{t}} - \sqrt{d_3t}\right)\right],$$

$$u_{15}(y,t) = \sum_{n=0}^{\infty}\left[Gm_2 erfc\left(\frac{d_9}{2\sqrt{t}}\right)\right],$$

$$u_{16}(y,t) = \sum_{n=0}^{\infty}\left[\frac{Gm_2}{2}\exp\left(d_4t + d_9\sqrt{d_4}\right)erfc\left(\frac{d_9}{2\sqrt{t}} + \sqrt{d_4t}\right) + \frac{Gm_2}{2}\exp\left(d_4t - d_9\sqrt{d_4}\right)erfc\left(\frac{d_9}{2\sqrt{t}} - \sqrt{d_4t}\right)\right],$$

$$u_{17}(y,t) = \sum_{n=0}^{\infty}\left[Gm_2 erfc\left(\frac{d_{10}}{2\sqrt{t}}\right)\right],$$

$$u_{18}(y,t) = \sum_{n=0}^{\infty}\left[\frac{Gm_2}{2}\exp\left(d_4t + d_{10}\sqrt{d_4}\right)erfc\left(\frac{d_{10}}{2\sqrt{t}} + \sqrt{d_4t}\right) + \frac{Gm_2}{2}\exp\left(d_4t - d_{10}\sqrt{d_4}\right)erfc\left(\frac{d_{10}}{2\sqrt{t}} - \sqrt{d_4t}\right)\right].$$

4. Results and Discussion

In this study, the unsteady flow of Casson nanofluid with the imposition of the magnetic field, porous medium, and heat- and mass-transfer effects is investigated and solved by utilizing the Laplace transform method. For further analysis of their effects on the velocity, temperature, and concentration propagation, a graphical illustration of Equations (20)–(22) is generated using Mathcad software. The numerical computation for the analytical solutions is performed by assigning the parameters to a selective value: $\phi = 0.02$, $\gamma = 1.5$, $M = 2$, $K = 0.5$, $Gr = 3$, $Gm = 5$, $\mathrm{Pr} = 21$, $Sc = 0.22$, and $t = 0.2$ [19,28]. Based on the study [19], Casson fluid is the relevant model for describing the properties of human blood. Therefore, it is worth noting that when using human blood as a base fluid, the Prandtl number is 21, $\mathrm{Pr} = 21$, which is very high compared to other common base fluids such as water, and it was adapted by Khalid et al. [29] and Saeed et al. [30].

Figure 2a,b and Figure 3 illustrate the impacts of ϕ on the nanofluid flow as well as on the thermal and solutal transfer propagation. According to Figure 2a, the resultant velocity escalates with every rise in the level of ϕ in both the case of SWCNTs nanofluid and MWCNTs nanofluid. Meanwhile, Figures 2b and 3 reveal that an elevation of ϕ raises the temperature of both CNTs nanofluids, and the reverse effect is reported for the concentration profile. The enhancement of the thermal boundary layer is caused by an increase in nanofluid thermal conductivity as ϕ rises. Physically, nanofluid thermal conductivity refers to the ability of a nanofluid to conduct or transfer heat, which implies that an increase in ϕ is equivalent to an increase in heat transfer or heat conduction by the nanofluid, resulting in a rising heat profile. Based on Equation (1), it is found that the velocity is temperature- and concentration-dependent, indicating that both the temperature and concentration of nanofluid will influence the propagation of the nanofluid velocity. As the temperature increases, the viscosity of nanofluid decreases due to the weakening of intermolecular forces between nanoparticles, and hence, the convective fluid flow increases [31]. For the concentration profile, an ascending ϕ provides insignificant changes to the profiles. However, the difference is clearly seen in the zooming box. Based on the results, it can be said that the use of nanofluids as a coolant agent can also be used in emergency cooling systems, where they can cool down overheated surfaces more quickly, leading to an enhancement in health and the healing process in the medical field and improved power-plant safety in the engineering field. A similar impact of ϕ can be found in the study by Noranuar et al. [19].

The distributions of both CNTs nanofluids' velocity affected by an increasing magnetic field M and porosity K are illustrated in Figure 4a,b. Amplifying the strength of M reduced the velocity of nanofluids. This effect is caused by the presence of the Lorentz force in the system, which provides an increase for a resistive force that eventually slows down the velocity of both SWCNTs and MWCNTs nanofluids. However, the velocity of nanofluids is enhanced by increasing the value of K. The presence of a porous medium reduced the resistance of the system, and the fluid could pass through the medium easily. From these results, it can be said that both the magnetic field and porous medium play important roles in the convective flow, where the flow can be stabilized and controlled by the presence of the magnetic field. Meanwhile, porosity diminishes the pressure inside a channel [32]. This creates attractive prospects for the use of magnetic fields and porosity factors in heat

exchangers and cooling devices. The impact of the same distribution of M and K on the velocity of nanofluid is also reported by Ramzan et al. [24].

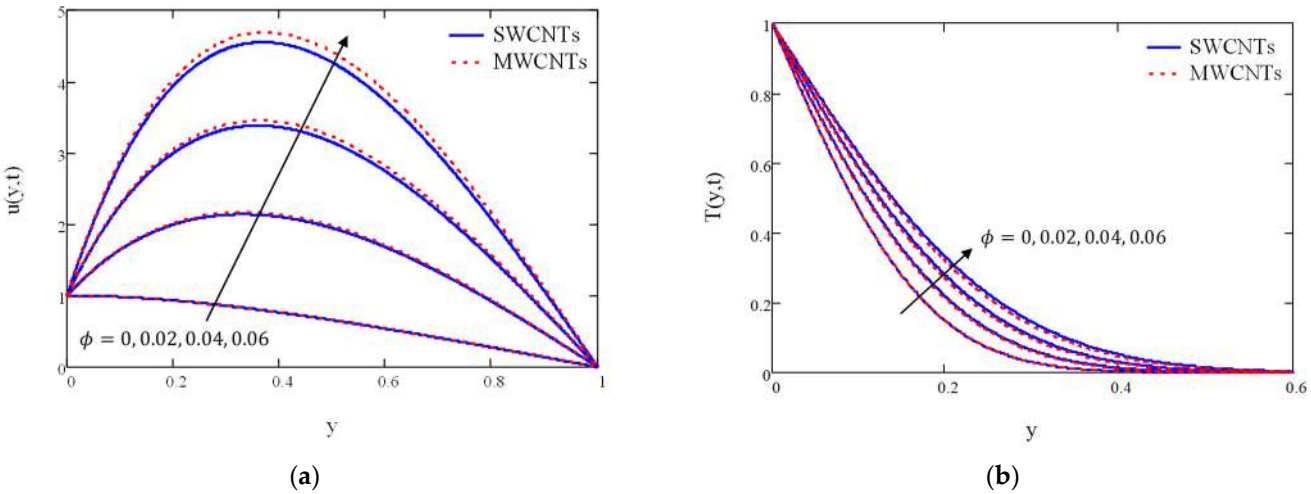

Figure 2. Profiles of (**a**) velocity and (**b**) temperature against ϕ.

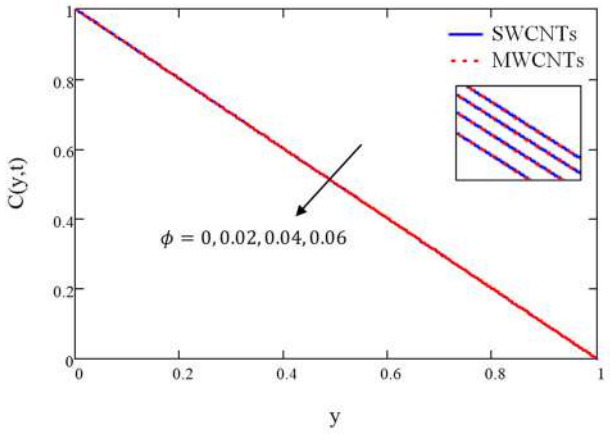

Figure 3. Profile of concentration against ϕ.

Figure 5a,b shows the impact of the Grashof number Gr and modified Grashof number Gm on the velocity of both CNTs nanofluids. Based on these figures, it is observed that the resultant velocity escalates gradually with increasing values of Gr and Gm. Both Gr and Gm play significant roles in free-convection phenomena, where their existence represents the proportion of buoyancy force and viscous force. Rising Gr and Gm imply the enhancement of the buoyancy force, which is able to induce the fluid flow. Physically, growing Gr and Gm are a way to oppose the resistive force (viscous force) in a system and promote the enlargement of velocity. These particular impacts of Gr and Gm can be justified with the study of Pattnaik et al. [1] and Roa et al. [2].

The influence of Pr on the temperature profile is demonstrated in Figure 6a, while the influence of Sc on the concentration profile is demonstrated in Figure 6b. The increasing value of Pr causes the temperature to decline. The same impact is shown on the nanofluid concentration when Sc is increased. In the heat-transfer problem, Pr is described as the proportion of momentum diffusivity to thermal diffusivity. Therefore, a high Pr value obtains a fluid with less thermal conductivity, resulting in a thin thermal boundary layer as well as a low heat profile. Meanwhile, Sc is the mass-transfer analogue of Pr, defined as the ratio of momentum diffusivity to molecular diffusivity. A high Sc value indicates that the fluid has less diffusivity of mass, which results in a thin concentration boundary layer as well as a low concentration profile. Likewise, both Pr and Sc produce the same effect on

the velocity profile, where their increase declines the velocity profile for both nanofluids, as shown in Figure 7a,b. Sehra et al. [6] and Abbas et al. [7] reported the same behavior of Pr and *Sc* on the velocity profile in their double convective study.

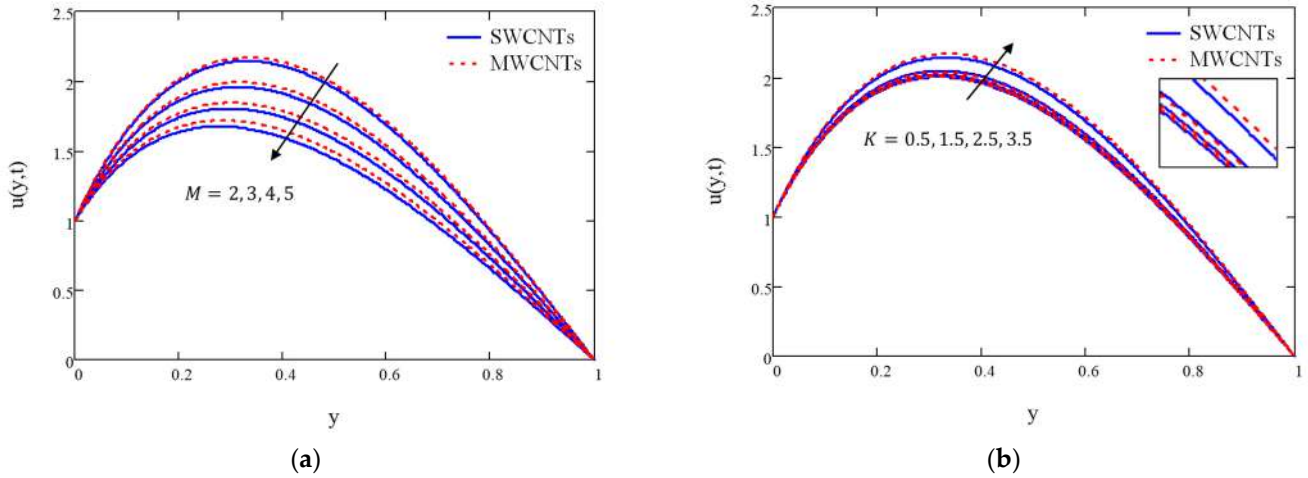

Figure 4. Profiles of velocity against (**a**) *M* and (**b**) *K*.

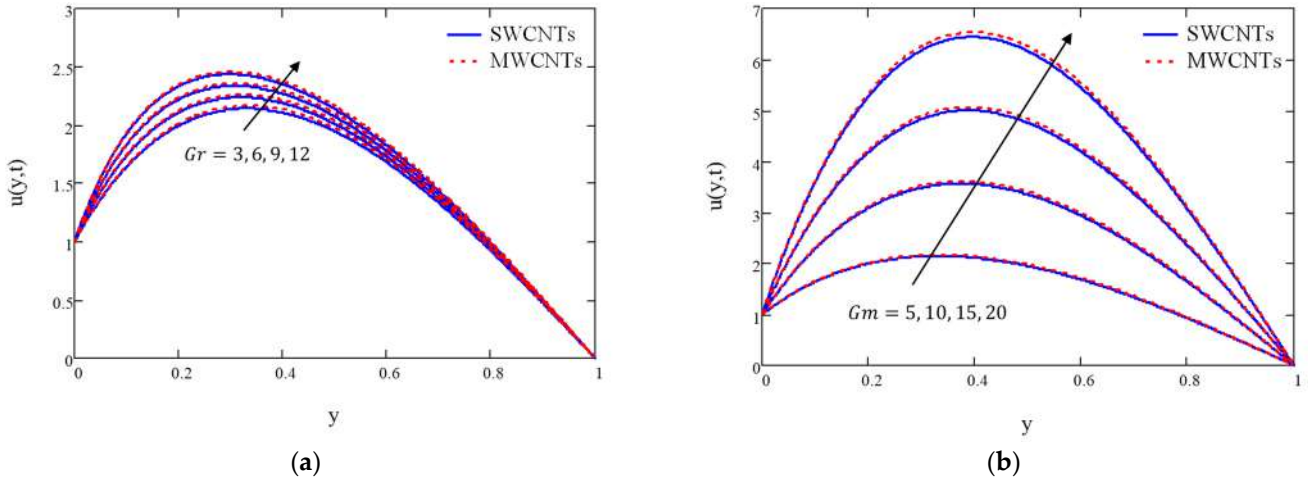

Figure 5. Profiles of velocity against (**a**) *Gr* and (**b**) *Gm*.

To control the accuracy of the results obtained, as seen in Figures 2–7 the propagation of all profiles satisfied the prescribed dimensionless boundary conditions for an asymmetrical channel from a cross-section with a cylindrical shape, as shown in Equations (13) and (14). Both CNTs' nanofluids seem to have an increasing trend when they move away from plate $y = 0$ and reach their maximum velocity in the range $0.3 \leq y \leq 0.4$. After that, the entire velocity will vanish as the nanofluids approach the plate $y = h$. The present analytical study may be very helpful among researchers in this field because the findings could be references for other numerical and experimental works and a guide for several industry sectors. However, many directions still require in-depth research, such as the effects of CNTs nanoparticles on convective fluid flow in a channel. In addition to future interest in the subject of nanofluid, the present study can be extended to the cylindrical coordinate system (blood-vessel applications) and apply hybrid nanofluid flow to various effects.

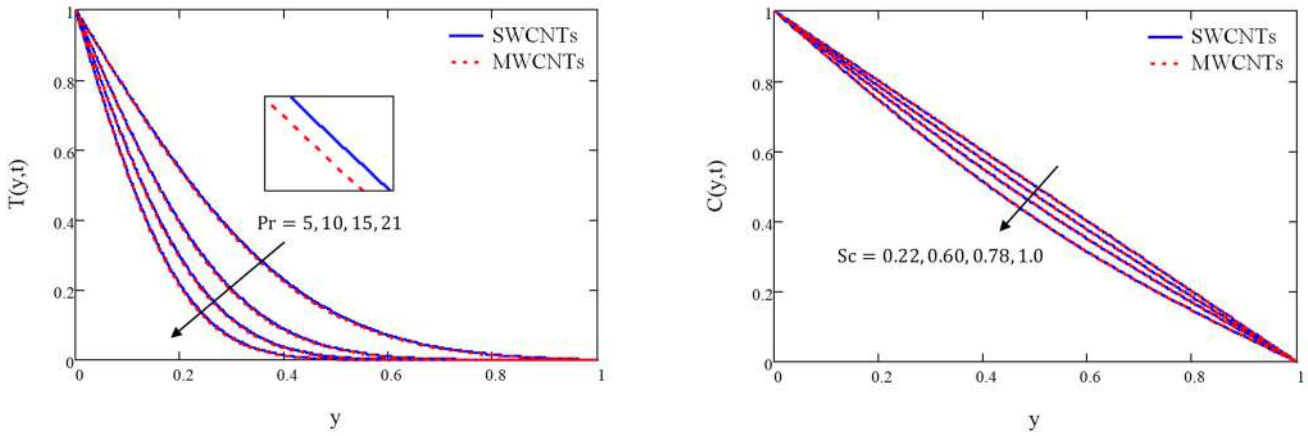

Figure 6. Profile of (**a**) temperature and (**b**) concentration against Pr and *Sc*.

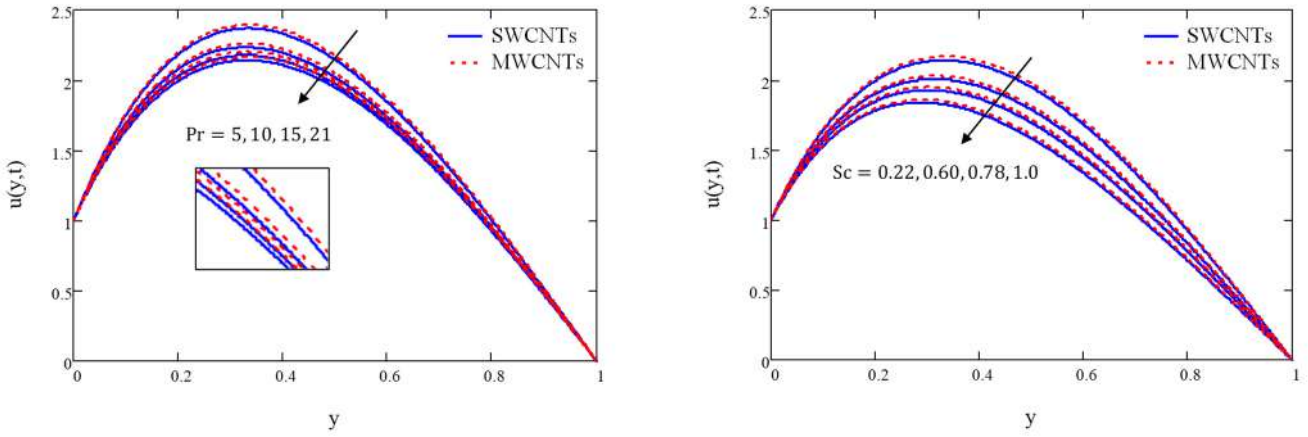

Figure 7. Profiles of velocity against (**a**) Pr and (**b**) *Sc*.

5. Conclusions

This article presented an analytical solution to an unsteady MHD Casson CNTs nanofluid flow passing through an asymmetrical channel embedded in a porous medium. The effects of heat and mass transport are taken into account, and the flow is induced by a moving vertical plate. This problem is tackled by the Laplace transform method. The impacts of the embedded parameters on the nanofluid velocity, temperature, and concentration are illustrated in graphs and discussed in detail. The findings show that the use of CNTs nanoparticles significantly enhanced both the velocity and temperature profiles compared to those without nanoparticles. This is because nanoparticles acted as the catalyst; their addition to the base fluid could boost the thermal conductivity of the nanofluid, which would lead to an efficient heat transfer. This plays an important role in heating and cooling systems, such as nanofluid coolants in the automotive sector, the extraction of geothermal power, nuclear reactors, and the cooling of microchips. The analysis of this analytical solution can be a reference for numerical and experimental works, as it could reduce the time and cost required to conduct an experiment as well as a numerical study validation.

Author Contributions: Conceptualization, W.N.N.N. and A.Q.M.; methodology, W.N.N.N.; software, W.N.N.N.; validation, W.N.N.N. and A.Q.M.; writing—original draft preparation, W.N.N.N.; writing—review and editing, A.Q.M., S.S. and L.Y.J.; visualization, W.N.N.N.; supervision, A.Q.M., S.S. and L.Y.J. All authors have read and agreed to the published version of the manuscript.

Funding: This research was funded by Universiti Teknologi Malaysia under Others Grant Scheme (R.J130000.7354.4B748) and Matching Grant Scheme (Q.J130000.3054.03M77).

Data Availability Statement: Not applicable.

Acknowledgments: The authors would like to acknowledge the financial support from Universiti Teknologi Malaysia for the funding under Others Grant Scheme (R.J130000.7354.4B748) and Matching Grant Scheme (Q.J130000.3054.03M77).

Conflicts of Interest: The authors declare no conflict of interest.

References

1. Pattnaik, J.R.; Dash, G.C.; Singh, S. Radiation and mass transfer effects on MHD flow through porous medium past an exponentially accelerated inclined plate with variable temperature. *Ain. Shams Eng. J.* **2017**, *8*, 67–75. [CrossRef]
2. Roa, S.R.; Vidyasagar, G.; Deekshitulu, G.V.S.R. Unsteady MHD free convection Casson fluid flow past an exponentially accelerated infinite vertical porous plate through porous medium in the presence of radiation absorption with heat generation/absorption. *Mater. Today Proc.* **2020**, *42*, 1608–1616.
3. Mohamad, A.Q.; Khan, I.; Shafie, S.; Isa, Z.M.; Ismail, Z. Non-coaxial rotating flow of viscous fluid with heat and mass transfer. *Neural Comput. Appl.* **2017**, *30*, 2759–2769. [CrossRef]
4. Noranuar, W.N.N.; Mohamad, A.Q.; Shafie, S.; Khan, I. Accelerated non-coaxial rotating flow of MHD viscous fluid with heat and mass transfer. *IOP Conf. Ser. Mater. Sci. Eng.* **2021**, *012044*, 1051. [CrossRef]
5. Zulkiflee, F.; Shafie, S.; Mohamad, A.Q. Radiation effect on free convection flow between oscillating parallel plates with mass diffusion. *Mal. J. Fund. Appl. Sci.* **2021**, *17*, 1–16. [CrossRef]
6. Sehra; Haq, S.U.; Shah, S.I.A.; Nisar, K.S.; Jan, S.U.; Khan, I. Convection heat mass transfer and MHD flow over a vertical plate with chemical reaction, arbitrary shear stress and exponential heating. *Sci. Rep.* **2021**, *11*, 4265. [CrossRef]
7. Abbas, S.; Nazar, M.; Nisa, Z.U.; Amjad, M.S.; Din, M.E.; Alanzi, A.M. Heat and mass transfer analysis of MHD Jeffrey fluid over a vertical plate with CPC Fractional derivative. *Symmetry* **2022**, *14*, 2491. [CrossRef]
8. Riaz, M.B.; Rehman, A.U.; Awrejcewicz, J.; Jarad, F. Double diffusive magneto-free-convection flow of Oldroyd-B Fluid over a vertical plate with heat and mass flux. *Symmetry* **2022**, *14*, 209. [CrossRef]
9. Afridi, M.I.; Qasim, M.; Makinde, O.D. Entropy generation due to heat and mass transfer in a flow of dissipative elastic fluid through a porous medium. *J. Heat Transf.* **2019**, *141*, 022002. [CrossRef]
10. Mahanthesh, B.; Gireesha, B.J.; Gorla, R.S.R. Heat and mass transfer effects on the mixed convective flow of chemically reacting nanofluid past a moving/stationary vertical plate. *Alex. Eng. J.* **2016**, *55*, 569–581. [CrossRef]
11. Madhura, K.R.; Babitha, S.S.I. Impact of heat and mass transfer on mixed convective flow of nanofluid through porous medium. *Int. J. Appl. Comput. Math.* **2017**, *3*, 1361–1384. [CrossRef]
12. Farooq, A.; Rehman, S.; Alharbi, A.N.; Kamran, M.; Botmart, T.; Khan, I. Closed-form solution of oscillating Maxwell nano-fluid with heat and mass transfer. *Sci. Rep.* **2022**, *12*, 12205. [CrossRef] [PubMed]
13. Siddique, I.; Sadiq, K.; Jaradat, M.M.M.; Ali, R.; Jarad, F. Engine oil based MoS2 Casson nanofluid flow with ramped boundary conditions and thermal radiation through a channel. *Case Stud. Therm. Eng.* **2022**, *35*, 102118. [CrossRef]
14. Arulmohzi, S.; Sukkiramathi, K.; Santra, S.S.; Edwan, R.; Gamiz, U.F.; Noeiaghdam, S. Heat and mass transfer analysis of radiative and chemical reactive effects on MHD nanofluid over an infinite moving vertical plate. *Results Eng.* **2022**, *14*, 100394. [CrossRef]
15. Prabavathi, B.; Reddy, P.S.; Vijaya, R.B. Heat and mass transfer enhancement of SWCNTs and MWCNTs based Maxwell nanofluid flow over a vertical cone with slip effects. *Powder Technol.* **2018**, *340*, 253–263. [CrossRef]
16. Sreedevi, P.; Reddy, P.S.; Chamkha, A.J. Magneto-hydrodynamics heat and mass transfer analysis of single and multi-wall carbon nanotubes over vertical cone with convective boundary condition. *Int. J. Mech. Sci.* **2018**, *135*, 646–655. [CrossRef]
17. Reddy, Y.R.O.; Reddy, M.S. Heat and mass transfer analysis of single walled carbon nanotubes and multi walled carbon nanotubes-water nanofluid flow over porous inclined plate with heat generation/absorption. *J. Nanofluids* **2019**, *8*, 1147–1157. [CrossRef]
18. Javed, F.; Riaz, M.B.; Iftikhar, N.; Awrejcewicz, J.; Akgül, A. Heat and mass transfer impact on differential type nanofluid with carbon nanotubes: A study of fractional order system. *Fractal Fract.* **2021**, *5*, 231. [CrossRef]
19. Noranuar, W.N.N.; Mohamad, A.Q.; Shafie, S.; Khan, I.; Jiann, L.Y. Heat and mass transfer in non-coaxial rotation of radiative MHD Casson carbon nanofluid flow past a porous medium. *Data Anal. Appl. Math.* **2021**, *2*, 37–51. [CrossRef]
20. Saqib, M.; Khan, I.; Shafie, S. Application of Atangana–Baleanu fractional derivative to MHD channel flow of CMC-based-CNT's nanofluid through a porous medium. *Chaos Solitons Fractals* **2018**, *116*, 79–85. [CrossRef]
21. Kumar, P.; Poonia, H.; Ali, L.; Areekara, S. The numerical simulation of nanoparticle size and thermal radiation with the magnetic field effect based on tangent hyperbolic nanofluid flow. *Case Stud. Therm. Eng.* **2022**, *37*, 102247. [CrossRef]
22. Rehman, S.U.; Ali, B.; Imran, M.; Ali, L.; Shah, N.H.; Chung, I.C. The Casson dusty nanofluid: Significance Darcy-Forchheime law, magnetic field, and non-Fourier heat flux model subject to stretch surface. *Mathematics* **2022**, *10*, 2887. [CrossRef]
23. Ali, L.; Ali, B.; Ghori, M.B. Melting effect on Cattaneo-Christov and thermal radiation features for aligned MHD nanofluid flow comprising microorganisms to leading edge: FEM approach. *Comput. Math. Appl.* **2022**, *109*, 260–269. [CrossRef]

24. Ramzan, M.; Nazar, M.; Nisa, Z.U.; Ahmad, M.; Shah, N.A. Unsteady free convective magnetohydrodynamics flow of a Casson fluid through a channel with double diffusion and ramp temperature and concentration. *Math. Meth. Appl. Sci.* **2021**, *1*, 1–20. [CrossRef]
25. Azmi, W.F.W.; Mohamad, A.Q.; Hoe, Y.S.; Isa, Z.M.; Shafie, S. Effects of Magnetohydrodynamics and Heat Transfer in Casson Fluid Through a Channel. *Mal. J. Fund. Appl. Sci.* **2021**, *17*, 416–429. [CrossRef]
26. Sadiq, K.; Siddique, I.; Ali, R.; Jarad, F. Impact of ramped concentration and temperature on MHD Casson nanofluid flow through a vertical channel. *J. Nanomater.* **2021**, *2021*, 3743876. [CrossRef]
27. Asifa; Kumam, P.; Shah, Z.; Watthayu, W.; Anwar, T. Radiative MHD unsteady Casson fluid flow with heat source/sink through a vertical channel suspended in porous medium subject to generalized boundary conditions. *Phys. Scr.* **2021**, *96*, 075213. [CrossRef]
28. Krishna, M.V.; Vajravelu, K. Rotating MHD flow of second grade fluid through porous medium between two vertical plates with chemical reaction, radiation absorption, Hall, and ion slip impacts. *Biomass Convers. Biorefinery* **2022**, 1–15. [CrossRef]
29. Khalid, A.; Khan, I.; Khan, A.; Shafie, S.; Tlili, I. Case study of MHD blood flow in a porous medium with CNTs and thermal analysis. *Case Stud. Therm. Eng.* **2018**, *12*, 374–380. [CrossRef]
30. Saeed, A.; Alsubie, A.; Kumam, P.; Nasir, S.; Gul, T.; Kumam, W. Blood based hybrid nanofluid flow together with electromagnetic field and couple stresses. *Sci. Rep.* **2021**, *11*, 12865. [CrossRef]
31. Apmann, K.; Fulmer, R.; Soto, A.; Vafaei, S. Thermal Conductivity and Viscosity: Review and Optimization of Effects of Nanoparticles. *Materials* **2021**, *14*, 1291. [CrossRef] [PubMed]
32. Farahani, S.D.; Amiri, M.; Majd, B.K.; Mosavi, A. Effect of magnetic field on heat transfer from a channel: Nanofluid flow and porous layer arrangement. *Case Stud. Therm. Eng.* **2021**, *28*, 101675. [CrossRef]